Mechanical and Fracture Characterization of 50:50 HDPE/PET Blends Presenting Different Phase Morphologies

L. Fasce, R. Seltzer, P. Frontini
Instituto de Investigaciones en Ciencia y Tecnología de Materiales, Universidad Nacional de Mar del Plata, Mar del Plata, Argentina

V.J. Rodriguez Pita, E.B.A.V. Pacheco, M.L. Dias
Instituto de Macromoléculas Professora Eloisa Mano, Universidade Federal do Rio de Janeiro, Rio de Janeiro, Brasil

Uncompatibilized and compatibilized blends of poly(ethylene terephthalate) (PET) and high-density polyethylene (HDPE) (50:50 PET/HDPE) have been prepared and characterized. A commercial grade of ethylene/methacrylic acid copolymer was used as compatibilizing agent and added to the blends in two different proportions, 1% and 7%. Compounded blends were processed following three different procedures: compression molding, extrusion, and extrusion followed by annealing. In every case, there is evidence that suggests that HDPE constitutes the matrix and PET is the dispersed phase. The PET phase shape was related to the processing procedure of the blends. PET adopted a globular morphology in the compression molded samples but it took the form of microfibers (microfibrillar-like reinforced composites) in extruded samples, which were flattened during the post-extrusion annealing process. According to the results obtained in tensile and fracture tests, extruded blends having 7% of ethylene/methacrylic acid copolymer appeared as the optimum combination of processing method and compatibilizer content. **POLYM. ENG. SCI., 45: 354–363, 2005.** **© 2005 Society of Plastics Engineers**

INTRODUCTION

Poly(ethylene terephthalate) (PET) and polyethylenes are extensively used in packaging of consumer and industrial products, being the most found in urban waste streams. One of the best ways of reducing urban waste is by recycling. Then, it would be highly convenient, in economical terms, to blend both polymers. The obstacle is that these two polymers are incompatible, i.e., PET and high-density polyethylene (HDPE) are immiscible in the liquid state and there is lack of adhesion in the solid state. The incompatibility of these two kinds of polymers, polyesters and polyolefins, gives rise to a "bad" morphology, gross separation and lack of adhesion between the phases. This is translated into poor mechanical performance, brittle behavior, and low barrier properties [1].

Compatibilization of incompatible blends leading to useful polymeric alloys is an attractive route to polymer property improvement and diversification [2–4].

A significant improvement of the morphology and of the mechanical properties, in particular of the elongation at break, of PET/HDPE blends can be achieved by using a third component acting as compatibilizing agent. The successful use of chemically different compatibilizing agents such as ethylene-vinyl acetate (EVA)- and ethylene-vinyl alcohol (EVOH)-based copolyesters, styrene-ethylene/butylene-styrene block copolymer (SEBS), grafted maleic acid SEBS (SEBS-g-MA), and ionomers, has been reported in the literature [1, 5–12]. A reduction of the interfacial tension of the compatibilized blend was reported, leading to size diminution of the dispersed phase and improvement of mechanical behavior of the polymer alloy, i.e., higher deformation at break.

The development of new multiphase blend materials depends primarily on two key requirements: control of interfacial chemistry and control of microstructures [13].

The compatibilization action of polyethylene-based ionomers in the PET/HDPE blend has been previously investigated by some of us [14]. Sodium and zinc based ethylene-methyl methacrylate acid copolymers containing 10% of the methacrylic comonomer with around 83% of the acid groups neutralized as Na and Zn carboxylate moieties were employed. When PET and these ethylene-methacrylic acid–based copolymers were processed in a mixer chamber,

Correspondence to: P. Frontini; e-mail: pmfronti@fi.mdp.edu.ar
Contract grant sponsor: CAPES (Brazil)–SECyT (Argentina); contract grant number: 039-01.
DOI 10.1002/pen.20282
Published online in Wiley InterScience (www.interscience.wiley.com).
© 2005 Society of Plastics Engineers

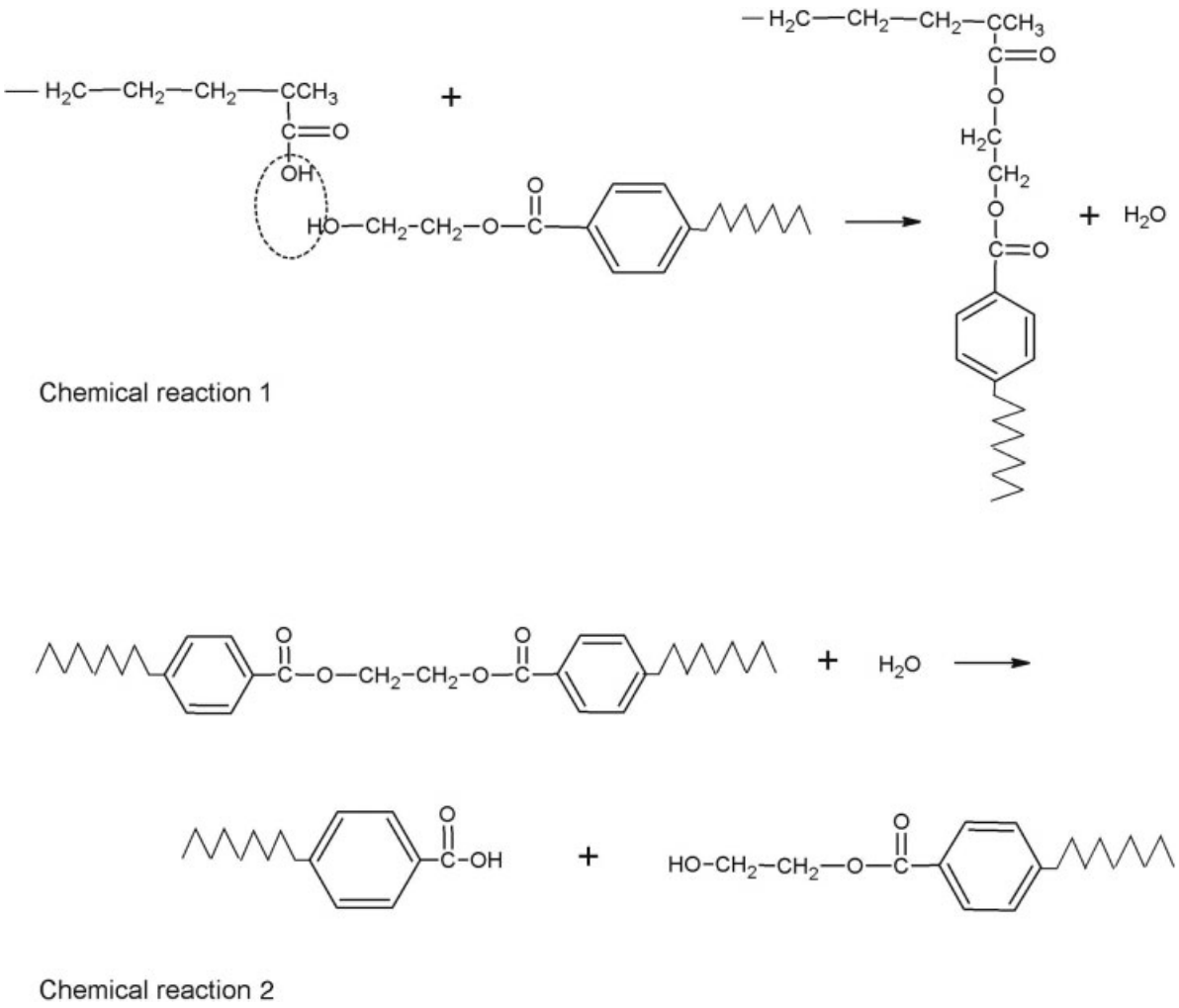

FIG. 1. Chemical reactions between PET and ethylene-methacrylic acid copolymers. Reaction 1: Reaction of EMA with hydroxyl PET chain end generating a grafting copolymer and water. Reaction 2: Reaction of water with ester groups forming acid and hydroxyl PET chain ends.

the initial blend torque increases with contact time, indicating an increase of molten state viscosity. This behavior was observed for partially neutralized copolymers (Zn- and Na-based ionomers) and for the ethylene copolymer containing only nonneutralized methacrylic acid counits. The increase of torque was associated with chemical reactions involving both polymers, which generates chemical species of higher molecular weights, probably grafting molecules constituted by ethylene chains with PET grafts (see chemical reaction 1 in Fig. 1). The reaction between the two polymers is accelerated by temperature and moisture, which attributed to an increase in hydroxyl end groups content generated by hydrolysis (see chemical reaction 2 in Fig. 1). Changing the processing temperature of a PET/ethylene-methacrylic acid copolymer 50/50 blend from 250 to 280°C, the torque increases from about 1 to 20 Nm in 20 min of blending. These copolymers were able to drastically modify the morphology of the blends obtained by extrusion, indicating that either the acid or the metal carboxylate is capable of faster reacting with the ester phase of the blend. The extent of these reactions will determine the degree of interaction between PET and HDPE phases in PET/HDPE blends containing these copolymers as third component.

In this study, virgin PET and HDPE were reactive blended using an ethylene/methacrylic acid copolymer (EMA) in different percentages as a compatibilizer agent to produce 50/50 PET/HDPE blends. The blends were processed following three different procedures: compression molding, extrusion, and extrusion followed by annealing (postextrusion annealing) to promote the formation of different morphologies. Afterward, their morphology, thermal properties, and mechanical behavior were studied.

MATERIALS, COMPOUNDING, AND SAMPLE PREPARATION

The materials used in this work were HDPE (Novatec JV060, T_m = 133°C, melt flow index = 6.1–8.0 g/10 min) provided by Polialden and PET (Polyclear T86, T_m = 244°C, inherent viscosity = 0.82 dl/g) provided by

Hoechst. Blends were compatibilized by reactive blending using an ethylene-methacrylic acid copolymer (EMA) (Nucrel 1202HC, acid content = 11%, melt flow index = 1.5 g/10 min, T_m = 99°C) provided by DuPont.

Before blending, the polymers were dried in an oven for 16 hours at 160°C (PET) and 60°C (acid copolymer). PET/HDPE blends were always prepared in 50/50 proportion and the amount of compatibilizer was 1 and 7 wt%; 50/50/xEMA pellets were compounded in a Haake Rheocord 9000 extruder at 280°C and 60 rpm. Investigation was carried out on blends prepared in three different ways. Compression molded plaques were obtained by compression molding the pellets (50/50/xEMA/C) at 270°C and 75 MPa during 15 min, followed by cooling with running water. Extruded ribbons were obtained from the same extruder by changing the die (50/50/xEMA/E). The temperature profile was 230, 260, 270, and 280°C in the four extrusion zones of the extruder and screw speed was 60 rpm. Molten extruded ribbons were quenched in a water bath at 30°C. Under this condition, PET developed a microfibrillar morphology in the molten state that was frozen in the HDPE matrix.

Part of the extruded ribbons were also annealed at 160°C under a pressure of 10 MPa for 15 min, followed by cooling with running water (50/50/xEMA/E_T), aiming to change the ribbons' structural properties [2].

EXPERIMENTAL

Differential scanning calorimeter (DSC) measurements were carried out in a Perkin Elmer Pyris 1 device equipped with a cooling accessory. Studied samples were obtained from the extruded blends. Nominal sample weight was 10 mg. The thermal cycle applied in the experiments consisted in a first heating at a scanning rate of 10°C/min from 35°C to 280°C, holding at 280°C for 3 min, cooling at 20°C/min from 280 to 35°C, and finally a second heating at 10°C/min. The first heating was made to erase the thermal history of the samples. The ability of PET to crystallize in the blend was evaluated from the cooling scan, while the bulk crystallinity of PET was determined from the second heating scan.

Mechanical tests were carried out at room temperature using an Instron 4467 universal testing machine on 1-mm-thick specimens machined from sheets processed in the three ways explained above. Extruded materials were always loaded in the processing direction and reported results are the average values of at least five specimens.

Tensile stress-strain curves were determined according to ASTM D638 M-82 recommendations at a crosshead rate of 5 mm/min on machined dumbbell specimens (type MII).

Fracture characterization was carried out on double edge-notched tensile specimens (DENT) cut from the compression-molded plates and ribbons (nominal width was 40 mm, nominal length was 80 mm, and ligament length to width ratio was 0.4), at a crosshead speed of 2 mm/min. Sharp notches were introduced by scalpel-sliding a razor blade having an on-edge tip radius of 0.13 mm. The stress intensity factor, K, for DENT specimens is as follows:

$$K = \frac{P}{B\sqrt{W}} f(a/W) \tag{1}$$

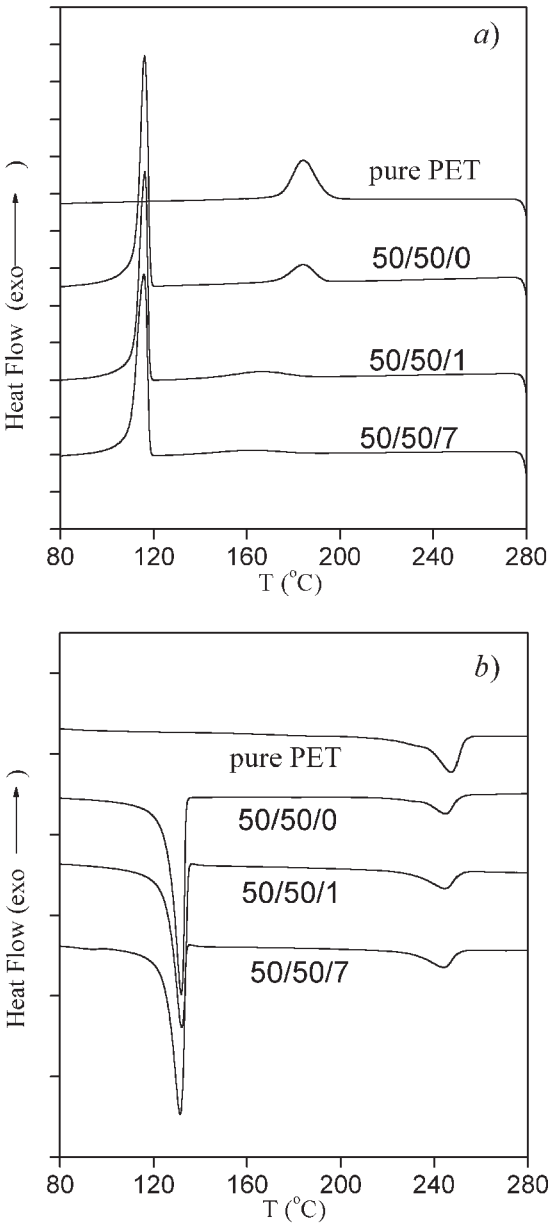

FIG. 2. DSC thermograms of blends as a function of EMA content. (a) Cooling scan. (b) Second heating scan.

TABLE 1. Calorimetric characterization of PET/HDPE/EMA blends.

	Cooling		2nd heating		
Material	T_c (°C)	ΔH_c (J/g)	T_m (°C)	ΔH_m (J/g)	X_c (%)
PET	184	38.5	247	36.5	30.4
50/50/0	184	36.1	245	37.6	31.3
50/50/1	161	20.5	244.4	37.7	31.4
50/50/7	≈160	Negligible	244	38.6	32.2

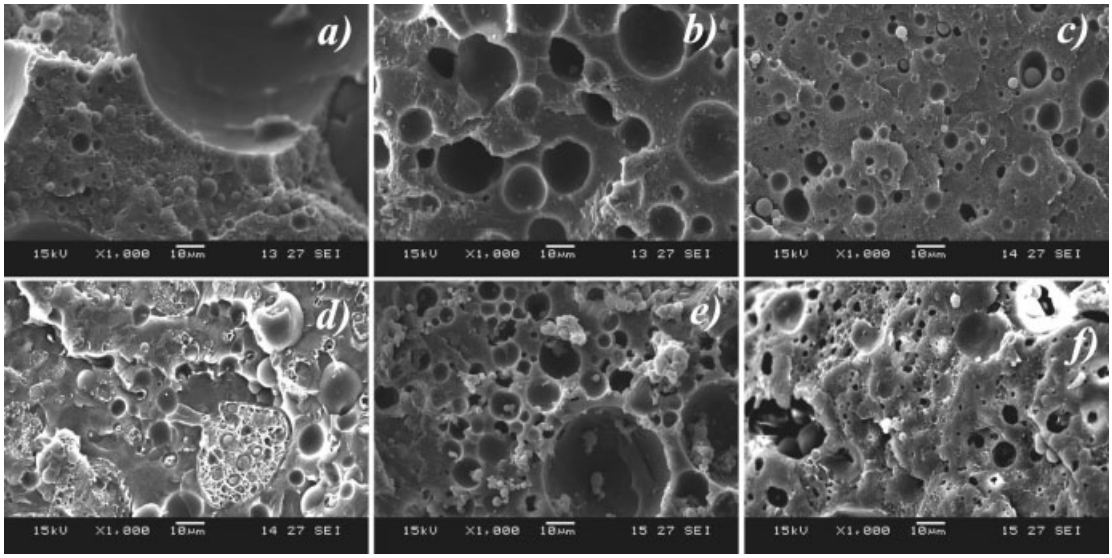

FIG. 3. SEM micrographs of cryofractured surfaces of PET/HDPE/EMA blends processed by compression molding: 50/50/0 (a) and 50/50/1 (d) without etching; 50/50/0 (b) and 50/50/1 (e) after xylene etching; 50/50/0 (c) and 50/50/1 (f) after phenol/trichlorobenzene etching.

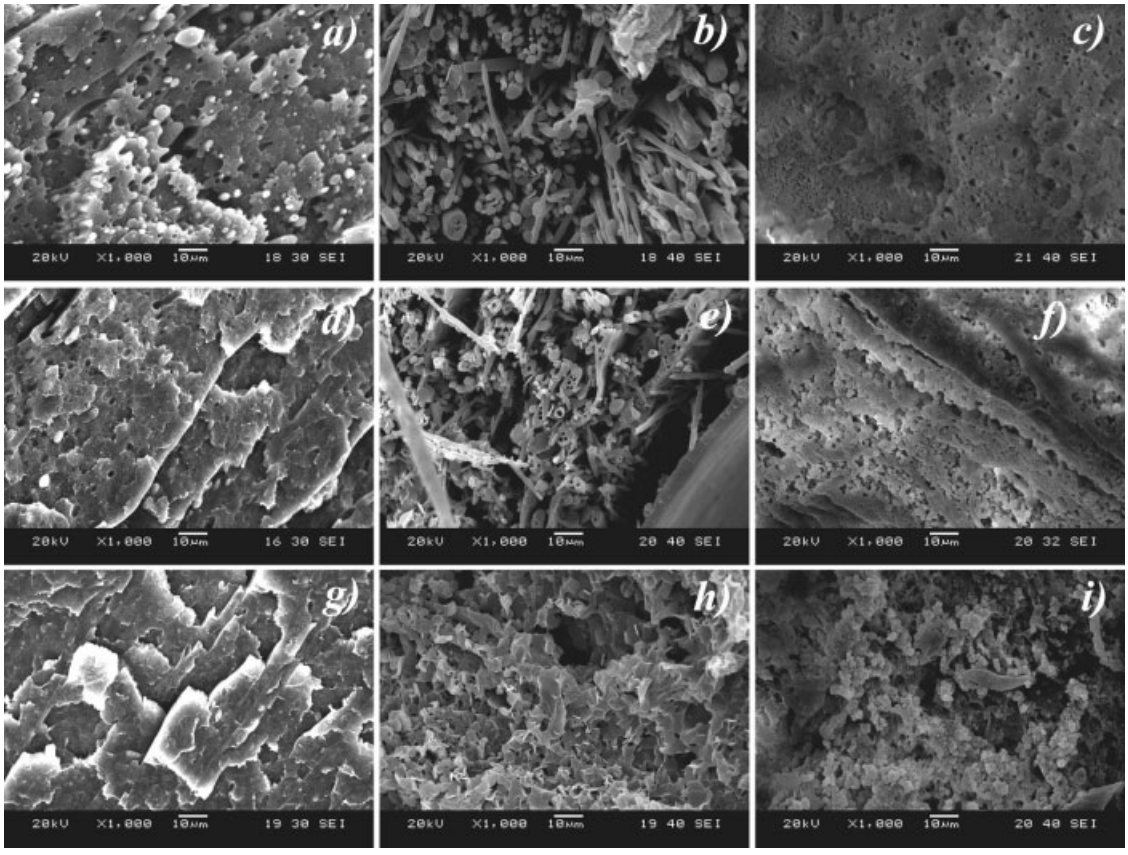

FIG. 4. SEM micrographs of cryofractured surfaces of PET/HDPE/EMA blends processed by extrusion: 50/50/0 (a), 50/50/1 (d), and 50/50/7 (g) without etching; 50/50/0 (b), 50/50/1 (e), and 50/50/7 (h) after xylene etching; 50/50/0 (c), 50/50/1 (f) and 50/50/7 (i) after phenol/trichlorobenzene etching.

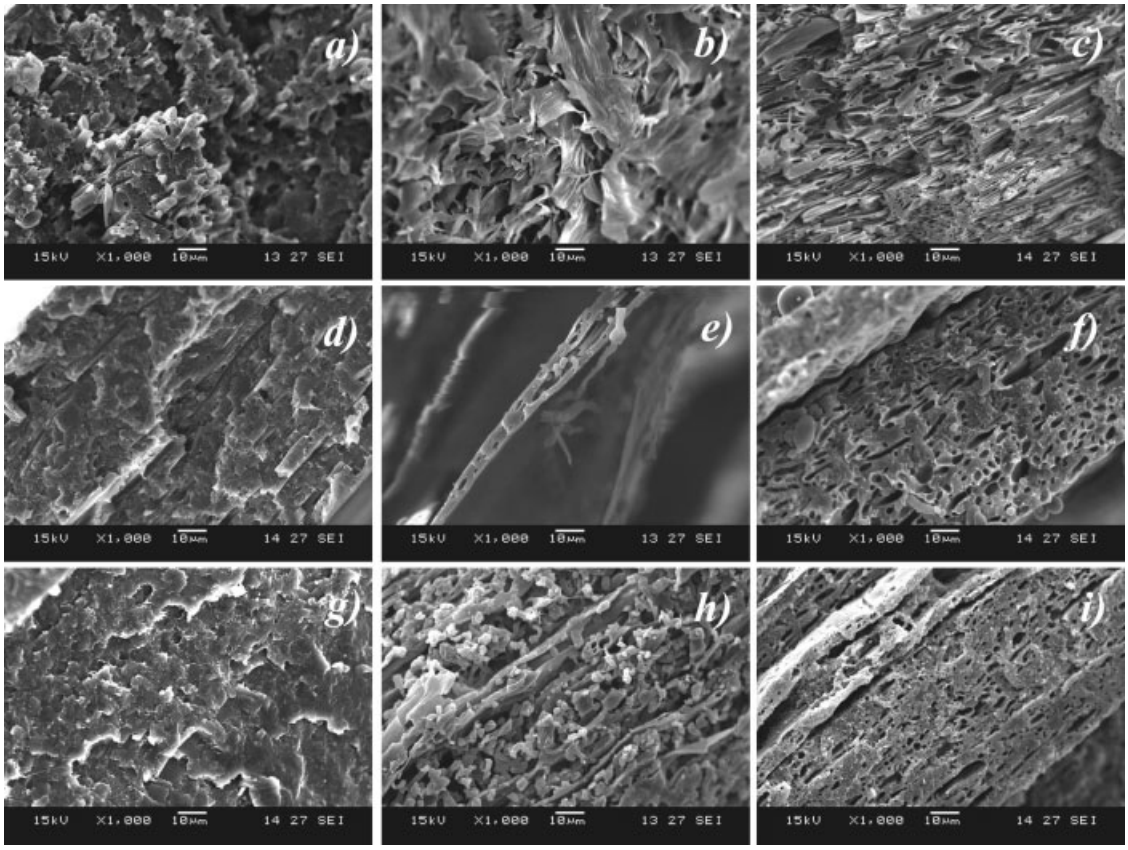

FIG. 5. SEM micrographs of cryofractured surfaces of PET/HDPE/EMA blends processed by extrusion followed by annealing at 160°C: 50/50/0 (a), 50/50/1 (d), and 50/50/7 (g) without etching; 50/50/0 (b), 50/50/1 (e), and 50/50/7 (h) after xylene etching; 50/50/0 (c), 50/50/1 (f), and 50/50/7 (i) after phenol/trichlorobenzene etching.

with

$$f(a/W) = \frac{\sqrt{\frac{\pi a}{2W}}}{\sqrt{1-\frac{a}{W}}}\left[1.122 - 0.561\left(\frac{a}{W}\right) - 0.205\left(\frac{a}{W}\right)^2 + 0.471\left(\frac{a}{W}\right)^3 + 0.19\left(\frac{a}{W}\right)^4\right] \quad (2)$$

where P is the critical load in the load-displacement trace, W is sample width, a is initial crack length, and B is the specimen thickness.

Scanning electron microscopy was carried out on a SEM (JEOL JMS-5300). Cryofractured specimens or etched surfaces were examined after coating them with a thin gold layer. To elucidate the phase morphology of the blends, selective solvent extraction were carried out on the fractured samples. Hot xylene was employed to extract HDPE from the fractured surface and PET was extracted from the sample surface by a mixture of phenol/1,3,5-trichlorobenzene (50/50 vol%).

RESULTS AND DISCUSSION

Based on the behavior of HDPE/ethylene-methacrylic acid copolymers reported in a previous work [14], it would be expected that the addition of small amount of EMA to a PET/HDPE blend would result in improvement of the level of adhesion between both incompatible phases. In this case, the product of the reaction between PET and EMA, which has segments compatible with HDPE and PET phases, may remain at the interfaces improving the interaction between the blend components.

Blend Crystallinity

DSC measurements were performed in order to evaluate the effect of the compatibilizer agent on the crystallization and melting behavior to PET/HDPE blends. Blend results are shown in Fig. 2, together with the trace obtained for a pure PET sample. Thermal properties of PET component in the blends are reported in Table 1, while the corresponding data for HDPE were not determined because of the onset at polyethylene crystallization temperature of PET cold crystallization. The degree of crystallinity (Xc) of PET component in the blends (Table 1) was evaluated as the ratio of its

measured enthalpy of fusion, normalized with respect to its weight fraction in the blend and divided by the enthalpy of fusion of the 100% crystalline PET (120 J/g).

In the first heating scan of the pure PET sample (trace not shown here) two characteristic peaks are observed, a crystallization exotherm (cold crystallization) occurred at 128°C and a melting endotherm at 247°C. During cooling, the crystallization peak is observed at 184°C and in the second heating scan only the melting peak at 247°C is evidenced.

During cooling, a HDPE crystallization peak is developed at 116°C for all blend compositions. Despite PET crystallization seems not to be influenced by the HDPE phase, the addition of the compatibilizer copolymer does alter PET crystallization (see crystallization peaks during cooling step in Fig. 2a). The latter results suggest the probable development of strong interactions between PET and copolymer. Similar results were reported for PET/HDPE blends compatibilized with a Zn-ionomer (a copolymer of ethylene and methacrylic acid partially neutralized with Zn) [15].

Two endothermic peaks characterize the melting behavior of the blends: one peak around 130°C, which corresponds to HDPE and the other at higher temperature, around 245°C, which belongs to PET. The average bulk crystallinity level achieved by PET component in the blends seems to be slightly affected by the blending process (Table 1).

Blend Morphology

Scanning electron microscopy (SEM) micrographs of liquid N_2 fractured samples are shown in Figs. 3–5 for compression molded, extruded, and postextrusion annealed blends, respectively.

Compression molded binary blend samples displayed a typical incompatible blend morphology, comprising discrete domains of the discontinuous component, and craters and voids left when particles attached only by weak mechanical adherence were pulled out during fracture. No evidence of interfacial interactions or adhesion between both components exists. However, the compatibilized blend shows practically no craters and a reduction in size of the globular separated domains (Fig. 3). From the deep observation of the phenol/trichlorobenzene etched specimens (see third column of micrographs on Fig. 3) it can be inferred that spherical PET domains constitute the dispersed phase. Compatibilized blend exhibits a finer dispersion of the PET phase, i.e., more particles of smaller dimensions, though some lack of homogeneity is still observed. Despite of blend composition (50/50) no signs of cocontinuous structure were displayed by SEM micrographs.

In the case of both extruded type samples, the compatibilized blend fracture surface appearance is clearly more even than the uncompatibilized one, which exhibits voids, caverns and pulled out particles (see first column of micrographs in Fig. 4 and also in Fig. 5).

Blend extrusion processing resulted in remarkable changes in the morphology. The etching of the specimens,

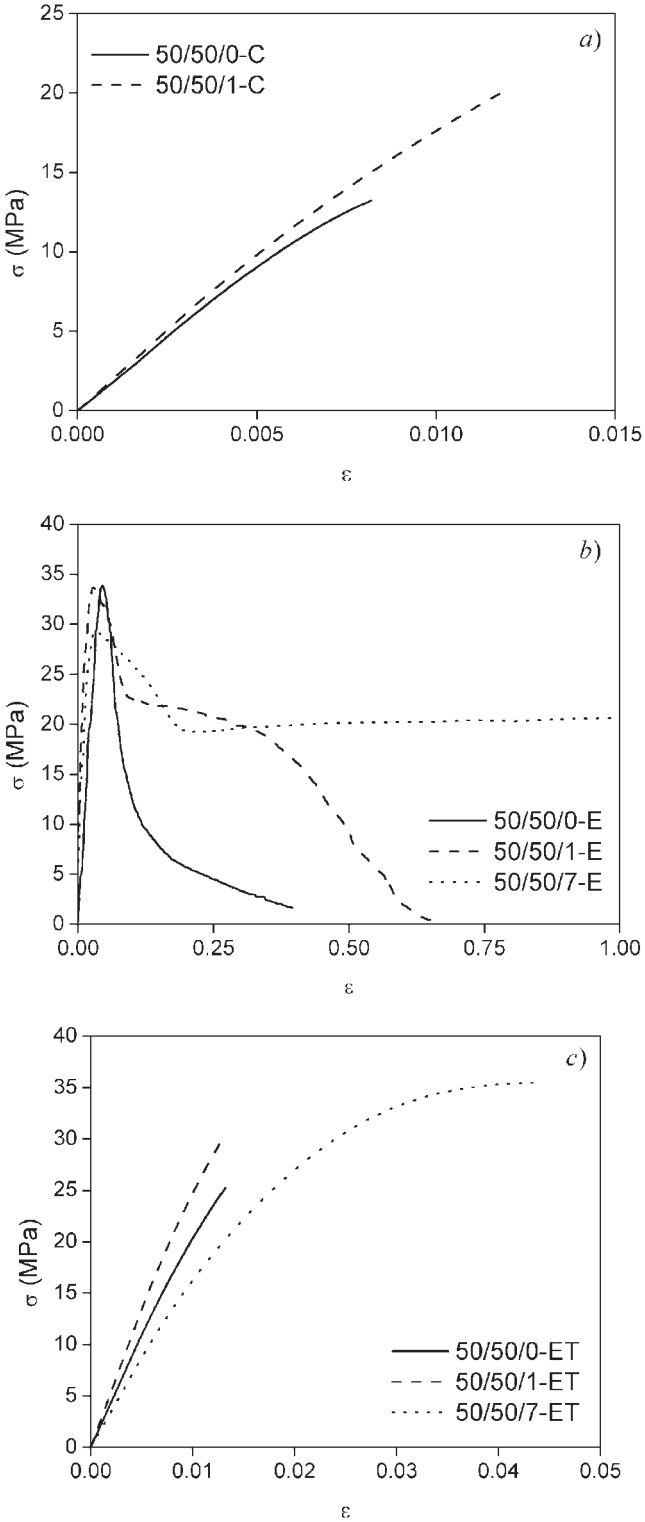

FIG. 6. Uniaxial tensile experiments performed on: compression molded samples (a); extruded samples (b); and postextrusion annealed samples (c).

where HDPE (second column of micrographs in Fig. 4) or PET (third column of micrographs in Fig. 4) phases were selectively removed, revealed a distinguishable fibrillated morphology. Microfibrils can be attributed to the PET dispersed phase, which appear suspended in the continuous HDPE matrix. The polymer fibrils were created during the

TABLE 2. Ultimate tensile properties and fracture toughness of PET/HDPE/EMA blends.

Material 50/50/	0EMA-C	1EMA-C	0EMA-E	1EMA-E	7EMA-E	0EMA-E_T	1EMA-E_T	7EMA-E_T
σ_u (MPa)	12.4 (±0.7)	21.8 (±1.7)	32.6 (±1.8)	34.7 (±1.4)	29.3 (±0.1)	28.4 (±4.5)	29.1 (±4.3)	33.5 (±3.4)
ε_u (%)	1.1 (±0.4)	1.2 (±0.1)	<10	60 (±49)	>125	2.2 (±1.1)	2.6 (±0.4)	3.9 (±1.5)
K_{max} (MPa.m$^{1/2}$)	0.90 (±0.03)	0.85 (±0.08)	1.56 (±0.08)	1.47 (±0.07)	1.47 (±0.12)	1.11 (±0.14)	1.29 (±0.07)	1.39 (±0.29)

drawing process of the polymer blend in the extruder, leading to the orientation and fibrillization of PET. Such microfibrillar structure has been reported to occur most readily at approximately equal fractions of the two components when both phases are near cocontinuous for similar [11, 16, 17] and other blends [18, 19].

As compatibilizer content increases, dissolution and extraction of HDPE from blend structure seems to become less effective. This fact revealed by the more interconnected morphological entities, evidences compatibilization between both phases.

The most striking characteristic displayed by postextrusion annealed samples is the lack of fibrillated structures in the SEM micrographs etched samples. It seems that the annealing treatment, which has been carried out without imposing a displacement restriction like in isotropization processes [20–24], disrupted fibrillated structure although blends were reprocessed far below the melting temperature of PET. Annealing treatment promoted a more lamellar type morphology of the HDPE continuous phase with flattened PET dispersed domains (Fig. 5).

Mechanical Performance

Tensile stress-strain curves were examined in order to reveal the effectiveness of compatibilization on tensile mechanical response. Typical stress-strain curves obtained for binary and ternary blends processed in the three different manners are plotted in Fig. 6. Large deformation tensile properties, ultimate strength and ultimate elongation, are reported in Table 2.

Compression molded and postextrusion annealed blends behave in a brittle way as shown in the normalized load-displacement traces (Fig. 6a and c). The elongation at break is indeed very low especially for compression molded samples, which also display very poor tensile strength in spite of the finer dispersion and improved solid-state adhesion generated by the compatibilizer. Such behavior is probably due to the development of higher crystallinity and spherulitic type crystals during annealing.

The stress-strain curves of the blends change drastically by adding 7% of EMA. Its addition significantly improves the elongation at break especially for the extruded nonannealed samples (see ϵ_u values in Table 2). Ultimate elongation is a property most sensitive to interfacial adhesion. The improvement in drawability promoted by EMA incorporation constitutes a clear sign of the formation of a strong interface layer capable of carry high shear stress levels during elongation process.

The improvement in the mechanical performance displayed by 7% EMA compatibilized extruded samples can be ascribed to the in situ formation of reinforcing microfibers. Necking initiation and necking propagation took place

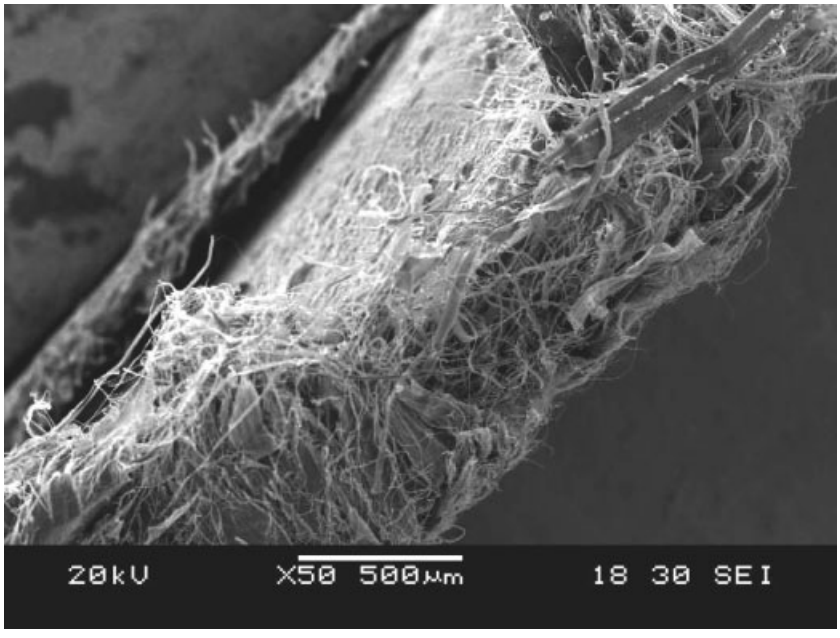

FIG. 7. SEM micrograph of the fracture surface of a uniaxial tensile 50/50/7 extruded sample.

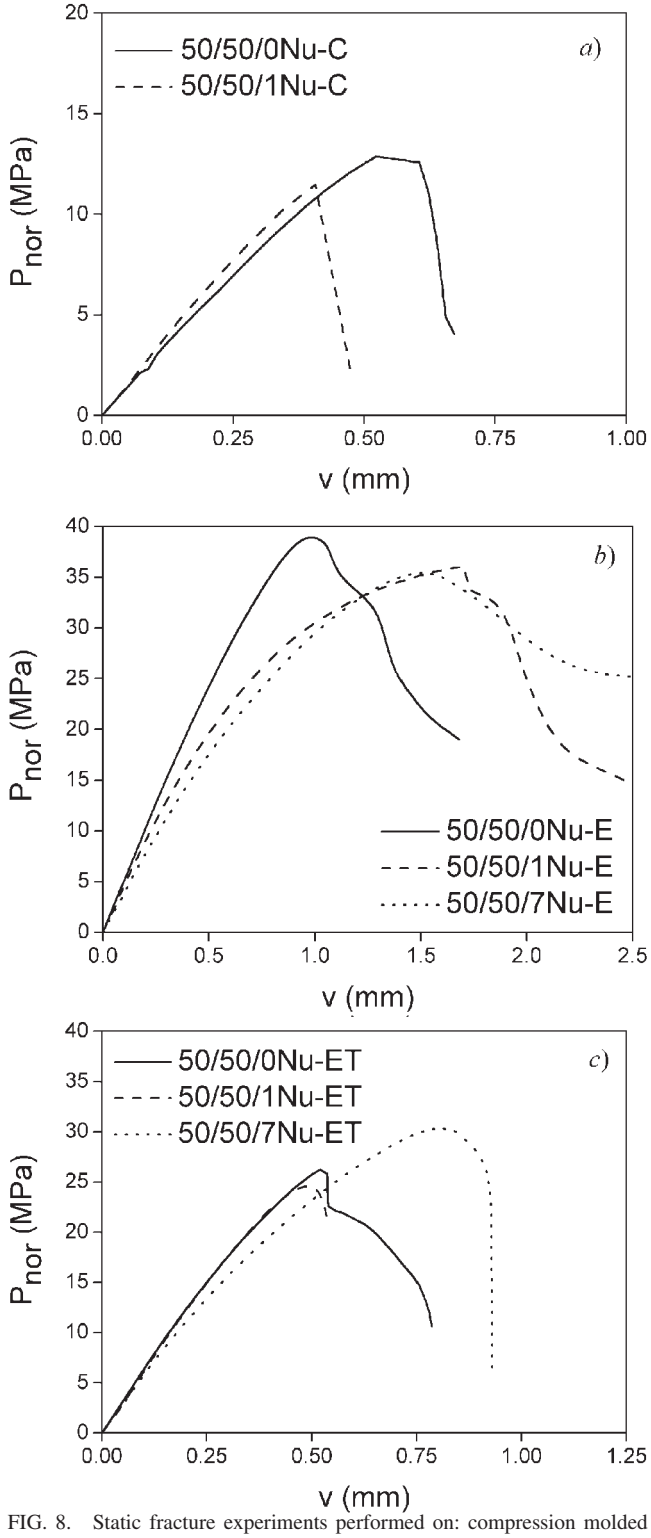

FIG. 8. Static fracture experiments performed on: compression molded samples (a); extruded samples (b); and postextrusion annealed samples (c).

thanks to the fiber pullout deformation micromechanism (Fig. 7).

The differences in the morphologies developed during processing were also reflected in fracture propagation modes. The fracture patterns displayed by the blends are presented in Fig. 8. As can be observed, these patterns were somewhat unusual to apply the standard protocols of fracture toughness evaluation. So the point of maximum stress was chosen as the boundary between crack initiation and crack propagation and, hence, the fracture toughness parameters were calculated according to *Eq. 1* at the maximum load (K_{max} values in Table 2).

Compression and postextrusion annealed specimens underwent brittle fracture. The force fell almost instantaneously from the maximum force to zero, displaying very low propagation energy. The highest K_{max} values were found for the extruded blends, which also present ductile fracture characteristics, defined here as a fracture process that requires additional energy to propagate a crack through the specimen. In every case, a tendency toward increasing final propagation displacement were found in coincidence with the increase in EMA copolymer content, which is expected to enhance interface strength.

Further insight in the investigation of fracture performance can be acquired from the detailed inspection of the side views of the already tested DENT specimens. Crack propagation patterns are shown in Fig. 9. It is clearly observed that both compression molded samples and postextrusion annealed ternary blends behave in a brittle manner and crack propagated through the ligament of the specimen. The postextrusion annealed binary blend does not present neat "in plane" crack propagation; the original crack is branched and deflected out of the plane that is normal to an applied uniaxial tensile stress due to the weak interface between the two phases and consequently the specimen is no longer loaded in a simple mode I.

On the other hand, crack advanced passing through the HDPE matrix and leaving PET fibers practically intact and available for load carrying in the binary and ternary extruded blends. This toughening mechanism, in which the fibers completely bridged the crack faces, preventing the blend from undergoing catastrophic failure, is known as a fully bridging situation [25]. After a certain degree of crack face displacement, fibers no longer bridge the crack faces and load starts to fall, while fibers are continuously pulled out from the matrix, allowing the composites to reach a higher level of final displacement.

Hence, the superior overall performance of the 7% EMA extruded compatibilized blend is based on the high degree of PET fibrillation, together with the stronger interface, giving rise to improved energy absorption capability with a sustained crack growth stability through crack surface bridging and large drawability. It clearly emerges that in the extruded sheets PET microfibrils act as anisotropic reinforcing elements distributed in the matrix.

Recently, other authors observed a similar type of distribution of the reinforcing elements in polymer blends [3, 18, 21, 24]. The "in situ" formation of the reinforcing species has led to the term "in situ composite" to describe materials of this type.

Our studies confirm the hypothesis, stating that morphology plays an important role in the mechanical properties of a polymer blend. A high degree of molecular orientation of

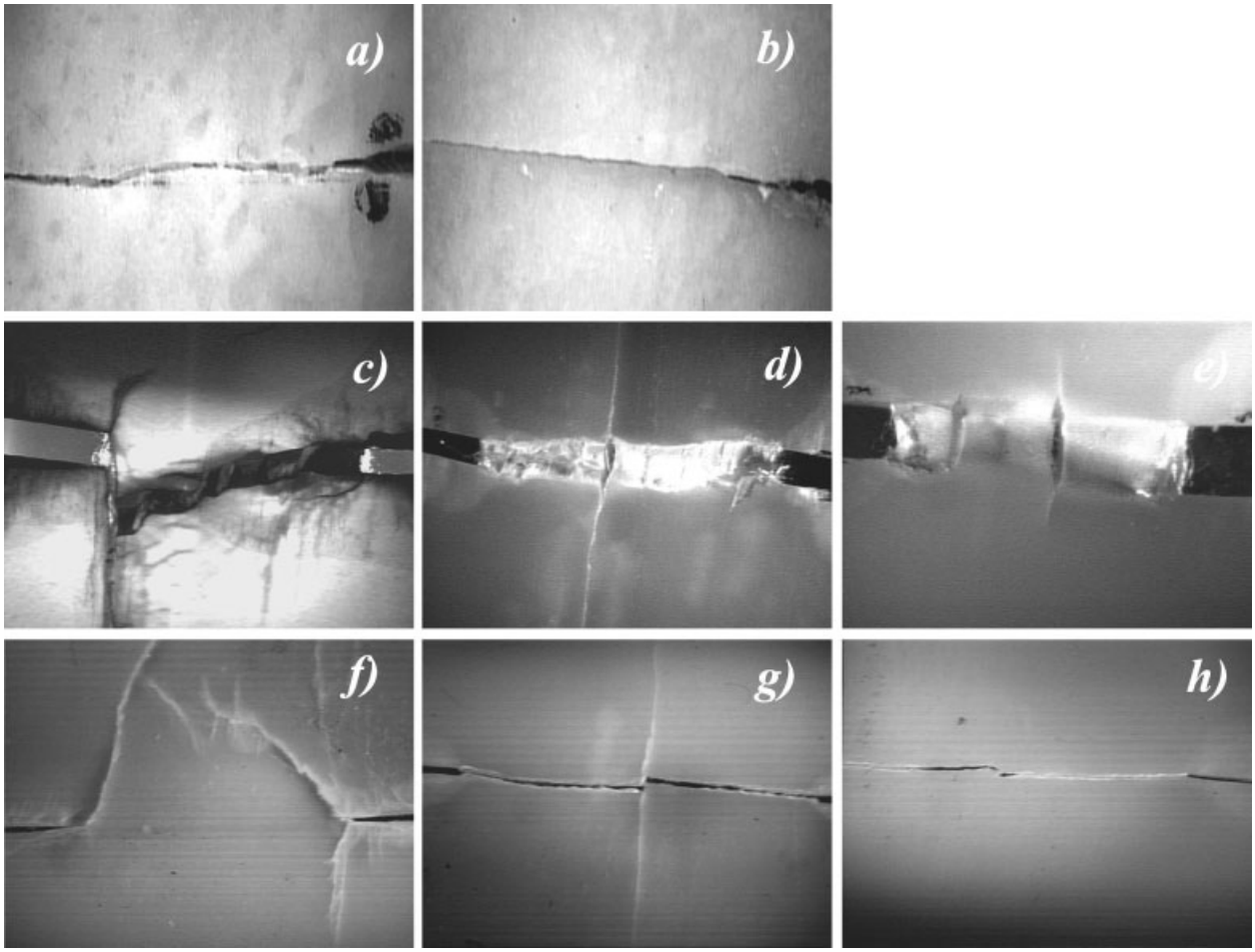

FIG. 9. Side view of the fractured specimens showing crack propagation path: 50/50/0-C (a); 50/50/1-C (b); 50/50/0-E (c); 50/50/1-E (d); 50/50/7-E (e); 50/50/0-E_T (f); 50/50/1-E_T (g); 50/50/7-E_T (h).

the reinforcing polymer may be essential in producing high-performance polymer alloys.

CONCLUSIONS

PET/HDPE are incompatible blends with poor mechanical properties. EMA copolymer can act as an effective compatibilizer when used as a third component at levels of approximately 7 wt%. Compatibilization was inferred on the basis of blend melt rheology [14], phase morphology, and mechanical properties.

A significant improvement of the mechanical properties, in particular of the elongation at break and fracture toughness, can be achieved by inducing fibrillation of the PET phase in the HDPE matrix by extruding the blends under adequate conditions. Processing techniques, like compression molding of extruded pellets, which are not capable of inducing fibrillation of the PET phase, lead to blends having poor mechanical properties.

The best overall properties were displayed by extruded blends compounded with 7% EMA. This is undoubtedly due to the details of the fibrillar morphology of the reinforcing domains, which promotes toughening by a fully bridged crack mechanism; and to the degree of adhesion at the interface due to compatibilization action of EMA, which confers the blends remarkable elongation capability.

In coincidence with other author's statements [5], extrusion of an incompatible polymer pair in which the dispersed phase forms in situ microfibers would be a preferable method to achieve appealing mechanical performance. Further work will focus on this latter issue.

REFERENCES

1. T.L. Dimitrova, F.P. La Mantia, F. Pilati, M. Toselli, A. Valenza, and A.Visco, *Polymer*, **41**, 4817 (2000).
2. L.A. Utracki, *Polymer Alloys and Blends*, Hanser, Munich (1989).
3. X.D. Lin and W.L. Cheung, *J. Appl. Polym. Sci.*, **88**, 3100 (2003).
4. C.K. Samios and N.K. Kalfoglou, *Polymer*, **40**, 4511 (1999).
5. J.C. Chen and I.R. Harrison, *Polym. Eng. Sci*., **38**, 371 (1998).
6. T.L. Carté and A. Moet, *J. Appl Polym. Sci.*, **48**, 611 (1993).

7. N.K. Kalfoglou, D.S. Scafidas, J.K. Kallistis, J.C. Lambert, and L.Van der Stappen, *Polymer*, **36**, 4453 (1995).
8. N.K. Kalfoglou, D.S. Skafidas, and D.D. Sotiropoulou, *Polymer*, **35**, 3624 (1994).
9. N.K. Kalfoglou and D.S. Skafidas, *Eur. Polym. J.*, **30**, 933 (1994).
10. C. Guerrero, T. Lozano, V. González, and E. Arroyo, *J. Appl. Polym. Sci.*, **82**, 1382 (2001).
11. Z.-M. Li, W. Yang, B.-H. Xie, S.Y. Yang, M.-B. Yang, J.-M. Feng, and R. Huang. *Mater. Res. Bull.*, **38**, 1867 (2003).
12. M. Pluta, Z. Bartczak, A. Pawlak, A. Galeski, and M. Pracella, *J. Appl. Polym. Sci.*, **82**, 1423 (2001).
13. B.D. Favis, in *Polymer Blends: Performance*, Vol. 1, Ch. 16 D.R. Paul and C.B. Bucknall, editors, John Wiley & Sons, New York, 501 (2000).
14. E.B.A. Pacheco and M.L. Dias, *J. Polym. Eng.*, **23**, 23 (2003).
15. A.M Arév and A.V. Sotonikov, *Vysokomol Soedin.*, **12**, 1799 (1970) [translated in *Polym. Sci. USSR*, **12**, 2040 (1970)].
16. Z.-M. Li, M.-B. Yang, J.-M. Feng, W. Yang, and R. Huang, *Mater. Res. Bull.*, **37**, 2185 (2002).
17. Z.-M. Li, M.-B. Yang, J.-M. Feng, W. Yang, and R. Huang, *Mater. Lett.*, **56**, 756 (2002).
18. M. Evstatiev, N. Nicolov, and S. Fakirov, *Polymer*, **37**, 4455 (1996).
19. P.L. Wajanakul, R. Pattanaolarn, J.W. Ellis, M. Nithitanakul, and B.P. Grady, *J. Appl Polym. Sci*., **89**, 620 (2003).
20. S. Fakirov, M. Evstatiev, and K. Friedrich, in *Polymer Blends*, Vol. 2, Ch. 33, D.R. Paul and C.B. Bucknall, editors, John Wiley & Sons, New York, 455 (2000).
21. M. Evstatiev and S. Fakirov, *Polymer*, **33**, 877 (1992).
22. S. Fakirov, M. Evstatiev, and J.M. Scultz, *Polymer*, **34**, 4669 (1993).
23. S. Fakirov, M. Evstatiev, and S. Petrovich, *Macromolecules*, **26**, 5219 (1993).
24. S. Fakirov and M. Evstatiev, *Adv. Mater*., **6**, 395 (1994).
25. E. Smith, *Int. J. Eng. Sci*., **27**, 1473 (1989).